Distribution of Chromium Contamination and Microbial Activity in Soil Aggregates

As a by-product of numerous industries, from wood preservatives to metal plating, chromium is an environmental carcinogen often found in some contaminated soils. Ideally, it can be fixed in place through a reaction that reduces a soluble form of chromium to an insoluble form. These processes have typically been analyzed by assuming microbial and chromium distributions are homogeneous within the soil. However, biogeochemical conditions within soils become heterogeneous at the scale where chemical transport is slow. This heterogeneity occurs in soil aggregates, millimeter-scale cohesive units comprised of many additional soil particles. Using an x-ray microprobe and micro-x-ray absorption near-edge structure (micro-XANES) mapping to examine soil aggregates at microscales, researchers from Lawrence Berkeley National Laboratory, The University of California, Berkeley, The University of Chicago, and the University of Georgia have shown that the heterogeneity of a complex system in nature will affect the efficiency of the chromium reduction: microenvironments exposed to oxygen and low in available organic carbon are oxidizing and therefore slow chromium reduction rates. These studies show that to understand the fate of chromium contamination can require analyzing chemical and microbiological distributions with microscale (micrometer to millimeter) spatial resolution.

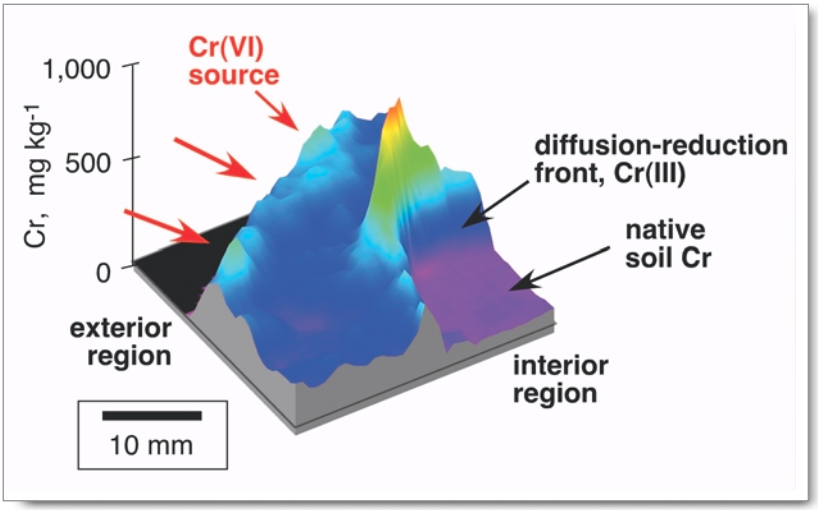

Fig. 1. Chromium distribution in a quarter-section slice through a natural soil aggregate, 31 days after exposure. Chromium occurs primarily as Cr(VI) along the exterior , and primarily as Cr(III) at the diffusion-reduction front.

Chromium VI (Cr(VI)) is soluble and easily transported through the environment. However, the natural soil microbial community can transform it to chromium III (Cr(III)) both directly, by enzymatic reduction, and indirectly, by depleting oxygen concentrations and increasing availability of iron II (Fe(II)), an important reductant in the soil. To analyze the efficiency of the microbial activity in reducing chromium, synthetic soil columns were examined, as were natural soil aggregates (both used Altamont clay, from Altamont Pass in Alameda County, CA). For the synthetic soil columns, the clay was homogenized and repacked into columns. The natural aggregates were simply collected as-is from the soil, in roughly spherical shapes, 90 to 150 mm across. Both columns and aggregates were permeated with a solution of Cr(VI) before fixing the aggregates by freezing, freeze-drying, and encasing in resin. (Half of the aggregates were fixed immediately after being exposed to the chromium; the other half were fixed 28 days later in order to study the soil after a month of microbial activity.)

The samples were mapped to obtain profiles of their chromium distributions. The synthetic columns were mapped over the course of a month by using x-ray microprobe and micro-x-ray absorption near edge structure techniques at the GSECARS beamline 13-ID at the APS. The natural aggregates were examined at Beamline X26A of the National Synchrotron Light Source, Brookhaven National Laboratory. Chromium reduction efficiency depended on the level of organic carbon available to the sample. Those samples that were enriched with carbon supported higher microbial activity and consequently very active reduction—organic carbon-rich, microbially active soils showed all the Cr(VI) reduced and immobilized as Cr(III). The distribution of oxygen had an effect as well, as oxygen inhibits chromium reduction. The maps showed that there was only Cr(III) on the inside of the samples with greater reduction, while only Cr(VI) was seen in the surface region, to depths of about a millimeter. The delineation between the two areas—a thin band where both types of chromium were present—was sharp, no greater than 0.2 mm in more microbially active soils. Such distributions of the two types of chromium could be seen within the first few days of the soil's first contact with the chromium solution; they were firmly established by the end of a month (Fig. 1). The heterogeneous nature of chemical and microbial composition of soil, therefore, has an obvious effect on immobilizing chromium that cannot be analyzed properly simply by averaging across the bulk samples.

The natural and synthetic samples showed surprisingly similar results, suggesting that synthetic columns are an effective laboratory tool, providing a good model for the natural system. Columns are useful since the window along the side of the container allows one to analyze the soil over time as the microbes are working, which cannot be done with natural aggregates.

Bulk analysis of contaminated soil systems — as well as any other samples — would simply show a mixture of Cr(VI) and Cr(III). This study shows, however, that this is not due sim-

ply to lack of complete reduction, but rather that the chromium is distributed in sharply differentiated areas, depending on microbial and chemical composition of the soil, thus still providing distinct areas of insoluble and immobilized Cr(III) and the more toxic Cr(VI). ❍

See: T.K. Tokunaga[1], J. Wan[1], T.C. Hazen[1], E. Schwartz[2], M.K. Firestone[2], S.R. Sutton[3], M. Newville[3], K.R. Olson[1], A. Lanzirotti[3], and W. Rao[4], "Distribution of Chromium Contamination and Microbial Activity in Soil Aggregates," J. Environ. Qual. **32**, 541-549 (March-April 2003).

Author affiliations: [1]Lawrence Berkeley National Laboratory, [2]University of California, Berkeley, [3]GSECARS, The University of Chicago, [4]University of Georgia

Funding provided through the U.S. Department of Energy Basic Energy Sciences, Geosciences Program, under Contract No. DE-AC03-76SF00098. The National Synchrotron Light Source, Brookhaven National Laboratory, is supported by the U.S. Department of Energy, Division of Materials Sciences and Division of Chemical Sciences. GSECARS is funded by the NSF (Earth Sciences Division) and by DOE (Geosciences Program). Use of the Advanced Photon Source was supported by the U.S. Department of Energy, Office of Science, Office of Basic Energy Sciences, under Contract No. W-31-109-Eng-38.

Properties of Iron Alloys Deep Inside the Earth

Understanding the composition of the Earth's core is one of the main challenges facing geophysicists today. From geochemical and planetary formation models it is believed that the main constituent of the core is an iron alloy with about 5% nickel by weight. Yet the density of the Earth's outer core is 10% lighter than pure iron at core temperatures and pressures. In addition, the velocity of sound waves in the outer core is 3% higher than in iron alone. These discrepancies are consistent with the presence of other chemical elements in the core structure. It is essential, therefore, that the effects of alloying on the physical properties or iron be measured in order to gather an accurate picture of the deepest parts of our planet. Recently, researchers from the Carnegie Institution of Washington, Argonne National Laboratory, and Academia Sinica in Taiwan used inelastic x-ray scattering (IXS) at the APS to measure the physical properties of iron-nickel and iron-silicon alloys at pressures comparable to Earth's core.

Among the elements that could be alloyed with iron in the core besides nickel, silicon stands out as a prime candidate light element. Other light elements, such as sulfur and oxygen, do not form solid solutions with iron in the relevant pressure and temperature ranges. Silicon, on the other hand, easily combines with iron to form alloys. To observe the effects of nickel and silicon on iron alloys, the researchers used nuclear resonant inelastic x-ray scattering (NRIXS) to measure the phonon density of states under high pressure. From the density of states, the velocity of sound waves—an important geophysical parameter directly measured by seismic wave study—can be derived.

Iron-57 was used in the creation of the test samples to single out the resonant x-ray absorption line for NRIXS. Samples of Fe-Ni were synthesized by reducing the starting elements in a hydrogen atmosphere at high temperature, followed by melting and annealing; the Fe-Si alloy samples were synthesized by arc melting. To conduct the measurements, alloy specimens together with a few ruby chips (an internal pressure calibrant) were placed in a hole drilled into a beryllium gasket which was put into a diamond anvil cell. The NRIXS measurements were carried out at X-ray Operations and Research beamline 3-ID at the APS in collaboration with staff from HP-CAT (APS sector 16).

Density-of-states profiles were calculated from the spectra at pressures up to 106 GPa for the iron-nickel alloy and up to 70 GPa for the iron-silicon alloy. To extract sound velocities, a parabolic fit was made to the low energy slope of the density of states curve. This yields a good approximation to the bulk Debye sound velocity of the samples containing iron-57. A correction factor was applied to obtain the sound velocities for the natural isotopic abundance. Aggregate compressional and shear velocities were then calculated with previously obtained equations of state for iron-rich nickel and silicon alloys as a function of density.

The results indicate that adding nickel to iron slightly lowers the compressional and shear velocities, whereas addition of silicon raises them, which is consistent with silicon being a major light element in the Earth's core. The results also indicate the importance of applying *in situ* x-ray microanalysis of this kind to geophysical problems, an application made feasible by the high brightness of third-generation synchrotron facilities such as the APS. The researchers have launched new experiments to understand the sound velocities and physical properties of iron and its alloys under extremely high pressures and temperatures by combining the NRIXS with the laser-heated diamond anvil cell technique. These state-of-the-art experiments will enable us to better understand geophysical and geochemical models of our planet's deepest part. ❍

See: J.-F. Lin[1], V.V. Struzhkin[1], W. Sturhahn[2], E. Huang[3], J. Zhao[2], M.Y Hu[4], E.E. Alp[2], H.-k. Mao[1], N. Boctor[1], and R.J. Hemley[1], "Sound velocities of iron-nickel and iron-silicon alloys at high pressures," Geophys. Res. Lett. **30**(21), 2112 (2003).

Author affiliations: [1]Carnegie Institution of Washington, [2]Argonne National Laboratory, [3]Academia Sinica, [4]HP-CAT and the Carnegie Institution of Washington

This work supported by tthe State of Illinois under HECA. We thank GSECARS and HPCAT, APS for the use of the ruby fluorescence system. Work at Carnegie was supported by DOE/ BES, DOE/NNSA (CDAC), NSF, and the W. M. Keck Foundation. Use of the Advanced Photon Source supported by the U.S. DOE, Office of Science, Office of Basic Energy Sciences, under Contract No. W-31-109-Eng-38.

Measuring Deformation Mechanisms at Pressures of the Lower Mantle

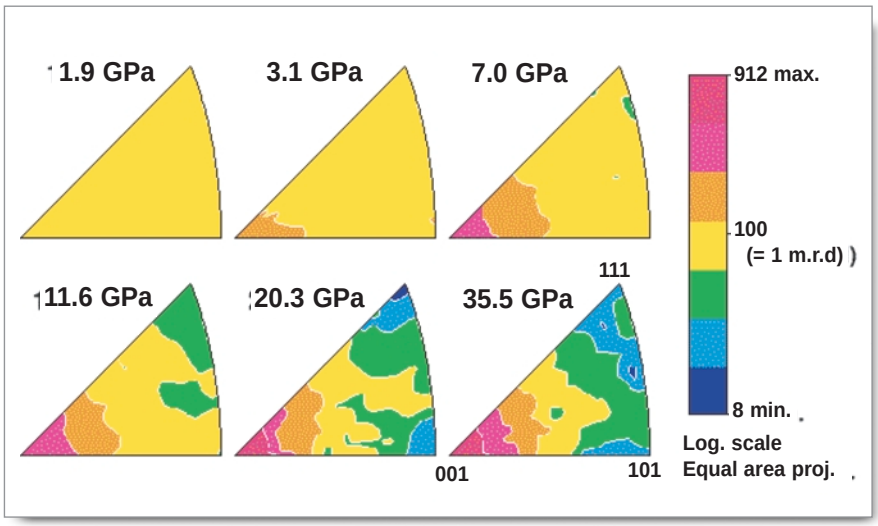

Fig. 1. Experimental inverse pole figures illustrating the development of lattice-preferred orientations in MgO over increasing pressures.

A deeper understanding the rheology of the Earth's mantle is important for understanding mantle convection and seismic anisotropy, but these studies are difficult to carry out in a laboratory setting due to the intense pressures needed. In addition, there are no good analogs for the minerals in question. Recent advances have been made, however, by using diamond anvils to put minerals under extreme pressures while performing x-ray diffraction. These methods have here been further improved by analyzing samples of polycrystalline MgO, commonly known as periclase. The data, collected by a group of researchers from École normale supérieure de Lyon, the Carnegie Institute of Washington, The University of California, Berkeley, and The University of Chicago, show the feasibility of analyzing elastic moduli, shear strength, and deformation mechanisms under pressures relevant to the Earth's lower mantle.

MgO was used in the samples because it is a common mineral, accounting for some 20% of the Earth's lower mantle. The MgO was ground down to particle sizes of about 1 μm and then pressed into platelets between two large diamonds. To pressurize the samples, a diamond anvil cell with a 300-μm-diameter tip was used, with a 65-μm hole drilled into the gasket to form a chamber for the sample. The chamber was filled with a layer of MgO powder, then a platelet of iron, then another platelet of MgO. Diffraction experiments were conducted by using angle-dispersive synchrotron x-ray diffraction at the GSECARS beamline 13-ID at the APS.

Samples were compressed from ambient pressure up to 47 GPa, at room temperature. As the pressure increased, the macroscopic deformation of the sample could be seen. The uniaxial stress component increased sharply from 0 to 7 GPa as the sample was raised from ambient pressure to 10 GPa. Above 10 GPa, the uniaxial stress component remained approximately constant at 8 GPa. For one set of samples in which the iron was not evenly placed, the uniaxial stress component then decreased as the iron underwent a phase transition at 12 GPa. The elastic moduli that were deduced were largely consistent with those derived from Brillouin spectroscopy. We observed progressive development of a sharp texture in the samples above 1.90 GPa, from which the calculated preferred lattice orientations were calculated and the active deformation mechanisms in the experiment were deduced.

In the context of the Earth's mantle itself, the data suggested that the single-crystal elastic anisotropy tends to decrease with pressure—although this effect is also countered by competing effects from increases in temperature. As such, the anisotropy factor decreases from 0.115 at 670-km depth to 0.050 at 1050-km depth, and then increases again to 0.180 at 1660-km depth. Results also suggest that polycrystalline MgO deforms by slip along the {110} system in cold compression up to the pressures found in the lower mantle.

While further study needs to be done on MgO to understand its behavior in the planet's interior, these raw results were in good agreement with results employing other techniques, which gives confidence that diamond anvil cells are an efficient way to analyze elasticity, strength, and deformation mechanisms in materials at extreme pressures. This is one of the first demonstrations that measurements of deformation mechanisms can be successfully done at pressures above 10 GPa. The transparency and immense pressure capabilities of the diamond anvil cells has opened new doors for studying minerals *in situ*, allowing for more realistic geodynamic models. ❍

See: S. Merkel[1,2], H.R. Wenk[3], J. Shu[2], G. Shen[4], P. Gillet[1], H.-k. Mao[2], and R.J. Hemley[2], "Deformation of polycrystalline MgO at pressures of the lower mantle," J. Geophys. Res. **107**(B11), 2271, 3-1 to 3-17 (2002).

Author affiliations: [1]École normale supérieure de Lyon, [2]Carnegie Institute of Washington, [3]University of California, Berkeley, [4]GSECARS, the university of Chicago

This work was supported by the National Science Foundation, the U.S. Department of Energy (DOE), the Center for High Pressure Research, the W.M. Keck Foundation, and the Centre National de la Recherche Scientifique-Institut National des Sciences de l'Univers program "Intérieur de la Terre." H.R.W. acknowledges support from NSF (EAR 99-02866), IGPP-LANL, the University of Chicago Education Abroad Program, and the A. von Humboldt Foundation. GSECARS is funded by the NSF (Earth Sciences Division) and by DOE (Geosciences Program). Use of the Advanced Photon Source was supported by the DOE Office of Science, Office of Basic Energy Sciences, under Contract No. W-31-109-Eng-38.

Measuring the Velocity of Sound in Diverse Materials

Measuring the velocity of sound through natural and fabricated compounds can reveal the composition and structure of materials at unprecedented detail. The challenge is to develop a method that can be used to determine sound velocity in condensed matter having a diverse structure. To overcome that challenge, researchers from the Carnegie Institution of Washington, Argonne National Laboratory, the University of Connecticut, and Northern Illinois University have applied nuclear resonant inelastic x-ray scattering — or NRIXS — at the XOR beamline 3-ID of the APS. Using NRIXS, they have successfully measured the velocity of sound in samples that represent both crystalline and noncrystalline materials [1]. Now that this method has been demonstrated successfully, researchers expect that it could significantly accelerate developments in high-pressure research and yield benefits in geophysics and other fields, like nanoscience.

NRIXS is used to study lattice dynamics of materials by means of low-energy nuclear resonances. Signals from nuclear resonance absorption are specific to the resonant isotope. Because the probe nuclei "see" the phonon excitation spectrum, researchers can extract the partial vibrational frequency distribution, which is a function often referred to as the partial phonon density of states (PDOS). NRIXS has been applied to diverse materials, including thin films and multilayers, nanoparticles, crystals with impurities, organic molecules, proteins, samples under high pressures, and geophysical samples. Most of these samples are compounds, and while the obtained PDOS gives only part of the lattice dynamics, the low-energy portion of the PDOS provides the Debye sound velocity of the whole sample.

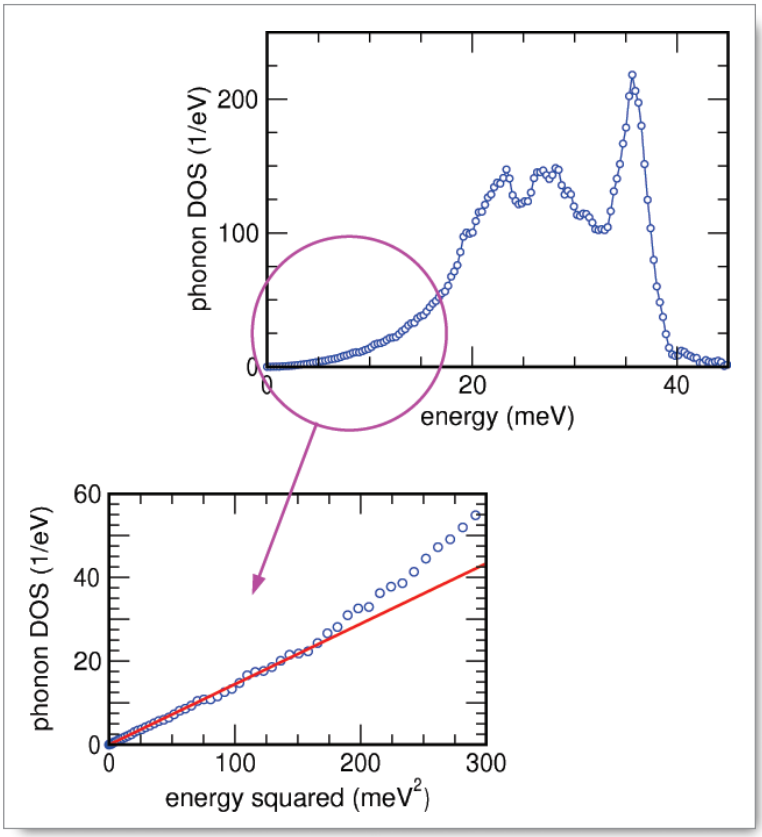

Fig. 1. Sound velocity can be derived from the low-energy part of the phonon densities of states. The quadratic behavior of the DOS in this region is usually a good approximation, which is demonstrated in the replot in the above figure.

In studies at the APS, researchers showed that, because of universal features of acoustic modes of harmonic solids, the low-energy portion of the PDOS is related to the Debye sound velocity. Specifically, they used NRIXS to measure the PDOS of a variety of samples. By averaging the PDOS of the samples, which were obtained from measured data from the PDOS in the region from 0 to 5 meV, researchers extracted numerical values for the velocities of sound (Fig.1). The results from NRIXS measurements of iron and palladium were within the range of sound velocities that were obtained by other means. But for hematite, the mean sound velocity, or vD, obtained by using NRXIS was lower than that obtained from measured elastic constants. One explanation for this difference may be that at the high frequencies used to derive sound velocity, phonon dispersion may be nonlinear, which could result in a lower vD. Improving energy resolution could make smaller phonon energies accessible, which would potentially provide a better measure of sound velocity. The technique is currently applicable to specific isotopes of Kr, Fe, Eu, Sn, and Dy, which can be present as an essential ingredient or doped as an impurity.

NRXIS is now poised to open new doors of scientific inquiry. Given its effectiveness—even for very low concentrations of nuclear resonant isotope — additional refinements are certain to lead to key developments in physical science. Not only does probing nuclei provide information about the host lattice, but strategically placing resonant nuclei in artificial structures may provide insight into local atomic motion, which at low energies is thought to influence the electronic noise in nanostructure devices. The NRIXS method is also promising in that it can complement other methods—or even replace established methods that are becoming too difficult to use. ❍

Reference

[1] See below.

See: M.Y. Hu[1], W. Sturhahn[2], T.S. Toellner[2], P.D. Mannheim[3], D.E. Brown[4], J. Zhao[2], and E.E. Alp[2], "Measuring velocity of sound with nuclear resonant inelastic x-ray scattering," Phys. Rev. B **67**, 094304-1 to 094304-5 (2003).

Author affiliations: [1]HP-CAT and Carnegie Institution of Washington, [2]Argonne National Laboratory, [3]University of Connecticut, [4]Northern Illinois University

Use of the Advanced Photon Source was supported by the U.S. Department of Energy, Office of Science, Basic Energy Sciences, under Contract No. W-31-109-Eng-38.

Mapping Impurities in Synthetic Diamond

With the advent of new growth methods, synthetic diamond has increasingly become an important technological material. As a result, a better understanding of the influence of impurities on the physical and chemical properties of diamond is essential. Impurities in natural diamond are of equal interest, because they can provide a record of gem growth and past environmental conditions. Among known impurities, metal atoms such as iron, nickel, and cobalt are the most common in synthetic diamonds. Over the past few decades, several experimental techniques have been brought to bear on the problem; however, these previous studies left unsettled questions owing to the limited capabilities of the experimental techniques used. Recently, a team of researchers from the Carnegie Institution of Washington, The University of Chicago, and Miami University used synchrotron x-ray fluorescence and absorption spectroscopy to study the behavior of iron and nickel impurities in synthetic diamond.

Commercial methods of diamond synthesis usually involve a high-pressure high-temperature (HPHT) process that employs iron and nickel as catalysts; hence their appearance as impurities in the finished material. Study of these impurities has been hampered by difficulties in preparing suitable samples. Because of the extreme hardness of diamond, creating a standard thin section of this material is problematic, and the necessary machining often causes high heat, which may alter the nature and distribution of metal impurities. In current work, GSECARS and HP-CAT researchers used the x-ray microprobe facility at GSECARS sector 13 at the APS to analyze impurities in as-grown synthetic HPHT diamond without the complications of post-synthesis processing.

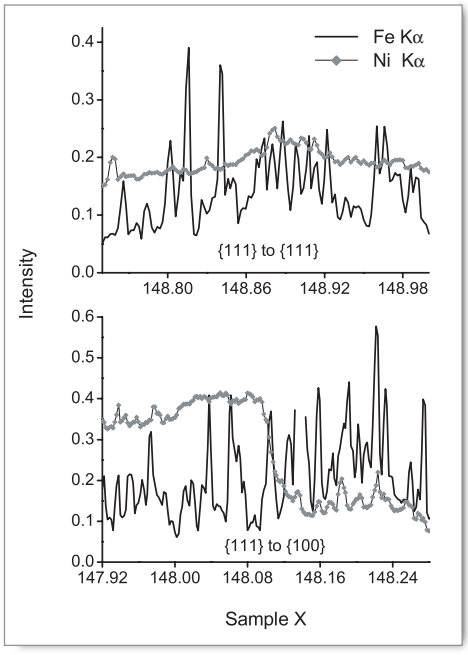

Fig. 1. XRF intensity of iron and nickel as a function of sample position. Top: Line scan with incident x-ray beam moved from a {111} sector to an adjacent {111} sector. Bottom: Line scan with beam moved across the boundary between a {111} sector and the adjacent {100} sector.

Fig. 2. Transmission and fluorescence tomograms. From the transmission data, the density of diamond (top) displays the orientation of the analyzed horizontal plane with four {111} faces and two {100} faces. Reconstructed iron and nickel fluorescence virtual slices are shown as labeled.

Diamond samples were selected from a commercial grit product of the General Electric Company. The grit was synthesized with iron and nickel catalysts under HPHT conditions, generally in the range from 1200˚C to 2000˚C and 5 to 7 GPa. Three crystals, each approximately 700 µm in diameter, were chosen for the study. X-ray fluorescence (XRF), x-ray tomography, and x-ray absorption near-edge structure (XANES) were used to analyze the diamond samples at 13-ID-C. In the XRF work, an incident beam energy of 8.6 keV was used, and Ka fluorescence lines from iron and nickel were collected with a multielement, energy-dispersive germanium detector. XANES scans were taken from 7040 to 7260 eV across the Fe K edge.

The XRF analysis showed a dramatic difference in the behavior of the iron and nickel impurities. The intensity pattern of the nickel Ka line indicates a dispersed distribution of nickel varying by sector throughout the sample, whereas the iron fluorescence shows sharp peaks as a function of position, consistent with aggregates or clusters of iron with no sector zoning (Fig. 1). The sector zoning of nickel is also clearly observed in the virtual slices reconstructed from the set of angular dependent line-scans (Fig. 2). In addition, it is possible from the XANES data to measure the oxidation state of the iron impurities in the diamond samples. Comparison with known iron compounds indicates that the iron in diamond has a valence of +2 in an octahedral coordination with FeO bonding.

Detailed atomic impurity studies such as these are made possible by the high brightness of the third-generation synchrotrons such as the APS, and by the energy and spatial resolutions of the spectroscopic instruments available at the GSECARS sector 13 at the APS. This advanced capability should be of special interest for future studies in a wide range of research fields, including geoscience, environmental science, gemology, materials science, and physical chemistry. ❍

See: Y. Meng[1], M. Newville[2], S. Sutton[2], J. Rakovan[3], and H.-k. Mao[1], "Fe and Ni impurities in synthetic diamond," Am. Mineral. **88**, 1555-1559 (2003).

Author affiliations: [1]HP-CAT and Carnegie Institution of Washington, [2]GSECARS, The University of Chicago [3]The University of Chicago

This work was supported byNSF, DOE, EAR-9814691, and the W.M. Keck Foundation. GSECARS is funded by the NSF (Earth Sciences Division) and by DOE (Geosciences Program). Use of the Advanced Photon Source was supported by the U.S. Department of Energy, Office of Science, Office of Basic Energy Sciences, under Contract No. W-31-109-Eng-38.

Phase Diagram of Tantalum at High Pressure

In materials science and geophysics, it is essential to understand how elements undergo the transition between solid and liquid phases at high pressures. For example, an accurate picture of materials performance under extreme conditions and detailed models of planetary interiors both depend on this knowledge. The element tantalum is especially interesting in this regard because it has one of the highest melting points at ambient pressure of any metal. At ambient temperatures, tantalum remains in a stable body-centered cubic (bcc) structure up to extremely high pressures. Tantalum therefore is a valuable test case for studying how materials melt. Despite a large number of experimental and theoretical efforts, however, agreement on the melting behavior of tantalum at high pressure has been elusive. Recently, researchers from the Carnegie Institution of Washington and the University of Valencia (Spain) have used the facilities of HP-CAT (sector 16) at the APS to obtain the phase diagram of tantalum at high pressure and temperature.

A number of previous experimental studies were carried out with the use of shock-wave measurements and laser-heated diamond anvil cells (DACs). Likewise, theoretical studies attempted to predict the melting curve of various materials. Unfortunately, substantial variation exists in the results of these earlier efforts, owing to the use of different experimental and theoretical techniques. Using the APS synchrotron and a laser-heated DAC, the researchers in the present study have gathered comprehensive melting data on tantalum over a wide range of pressures.

Commercial tantalum powder was used in the experiments. It was loaded into the pressure cell with sodium chloride as the pressure-transmitting and thermally insulating medium. Fluorescence from a ruby chip and the shifts in the sodium chloride x-ray diffraction lines were used to determine the cell pressure. The samples were heated on both sides of the cell by means of two infrared Nd:YLF lasers, and the temperature distribution was measured by spectroscopic imaging of the thermal radiation from the hot cell. X-ray diffraction measurements of the samples in this cell were made at the HP-CAT beamline 16-ID-B. The beam was filtered with a double-crystal monochromator to a wavelength of 0.3738 Å having an energy resolution of 10^{-3}. Diffraction patterns were recorded with a charge coupled device array and corrected for distortion.

The research team successfully performed experiments at pressures up to 52 GPa and temperatures as high as 3800K. Pressure-temperature data were obtained by compressing the samples to a desired pressure and then heating them. The melting point was ascertained by the disappearance of the tantalum diffraction lines (Fig. 1) and the appearance of a diffuse broad scattering for nine different pressure values. Thermally induced pressure changes were estimated by the shifts in the NaCl diffraction lines. The P-T measurements (Fig. 2) agree well with earlier DAC experiments but differ with previous observations performed with a piston-cylinder pressure chamber. Moreover, the present results do not follow an empirical Lindemann relation but rather can be understood with the help

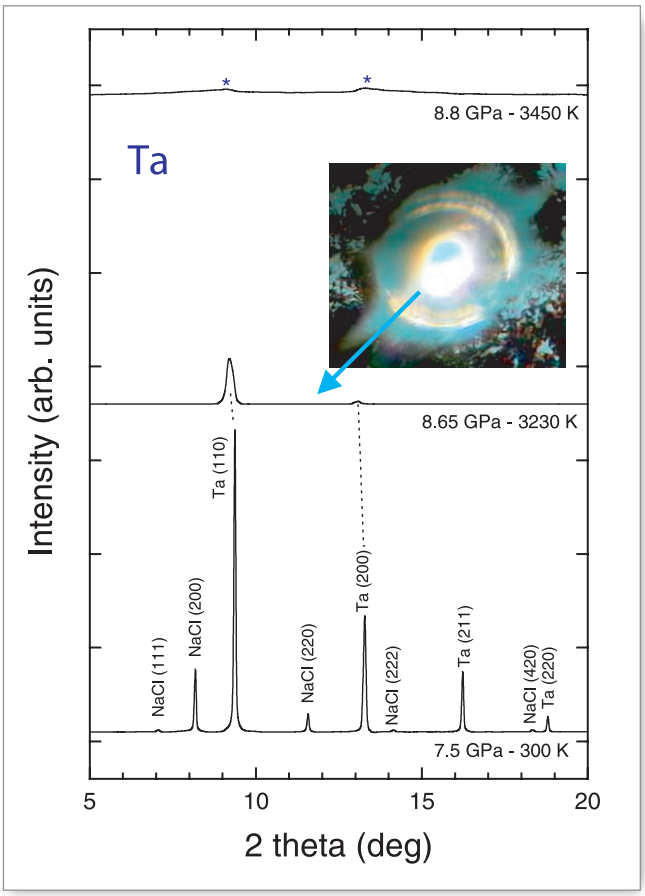

Fig. 1. X-ray diffraction patterns (λ = 0.3738 Å) in a tantalum sample at different temperatures around 8 GPa. P and T are indicated in the figure, and the diffraction peaks are identified. Stars depict the broad scattering characteristic of the onset of melting. The inset shows a hot tantalum sample from which the 8.65 GPa, 3230K pattern was measured.

of a vacancy generation model of melting. From these measurements, a pressure-volume-temperature (P-V-T) equation of state for tantalum was obtained.

These results indicate the importance of microstructural analysis and careful temperature mapping in obtaining accurate P-T data at high temperatures and pressures. In part, this type of measurement is made possible by the high brightness and precise energy resolution available at the APS. Currently, research in this area concentrates on extending the studies on Ta and other bcc transition metals (e.g., Mo and W) to the megabar (100 GPa) pressure range searching for the existence of a predicted unknown high P-T phase. ❍

See: D. Errandonea[1,2], M. Somayazulu[1], D. Häusermann[1], and H. K. Mao[3], "Melting of tantalum at high pressure determined by angle dispersive x-ray diffraction in a double-sided laser-heated diamond-anvil cell," J. Phys. Condens. Matter **15**(45), 7635-7649 (2003).

Author affiliations: [1]HP-CAT/Carnegie Institution of Washington, [2]Universitat de València, [3]Carnegie Institution of Washington

This work was supported by the NSF, the DOE, and the W M Keck Foundation. D.E. acknowledges the financial support from the MCYT of Spain and the Universitat of València through the 'Ramón y Cajal' program for young scientists. Use of the Advanced Photon Source was supported by the U.S. Department of Energy, Office of Science, Office of Basic Energy Sciences, under Contract No. W-31-109-Eng-38.

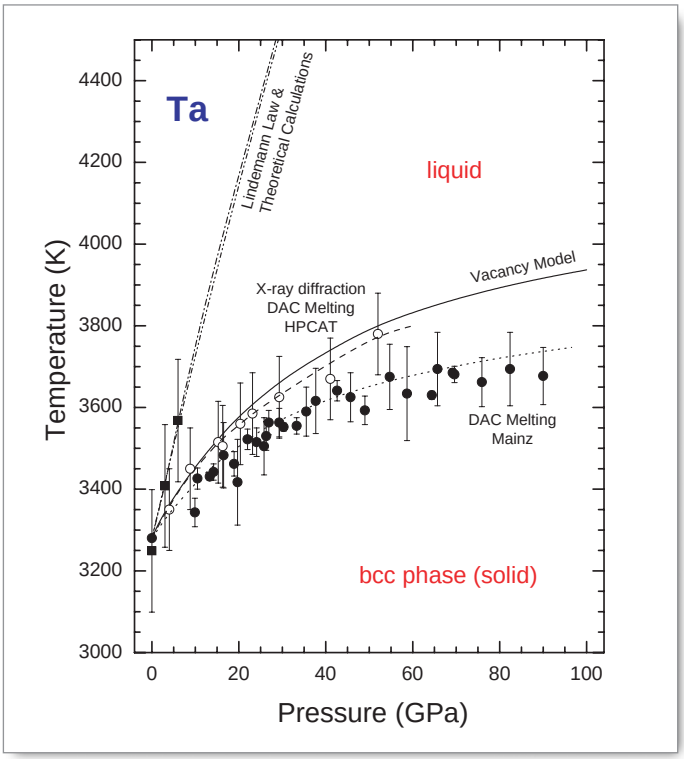

Fig. 2. P-T phase diagram of tantalum. Present synchrotron data (open circles) and previous data (solid circles and squares) are shown together with theoretical estimations. The dashed and dotted lines are fits to the experimental data. The solid line is the melting calculated by Errandonea et al. by assuming a vacancy-mediated melting model.

Getting the Lead out: Sorption vs. Biomineralization in *B. cepacia* Biofilms

Lead is one of the most common toxic heavy metals found in contaminated soil sites, but it can be fixed in place through sorption to metal oxide surfaces, as well as through biomineralization because of the microbial community. Using x-ray spectroscopy methods, researchers from Stanford University, The University of Chicago; Pacific Northwest National Laboratory, and the Stanford Synchrotron Radiation Laboratory studied biofilms of *Burkholderia cepacia*, a ubiquitous bacteria, to examine its mode of Pb (II) uptake — important information because the chemical form of Pb in the soil affects its solubility, bioavailability, and toxicity. For example, Pb that has been biomineralized will be more firmly fixed in place than that which is solely sorbed, since environmental changes, such as changes in pH, can lead sorbed metals to be re-released into the soil. These studies showed that biomineralization accounts for 90% of the total Pb immobilization below pH 4.5, but only 45-60% at near-neutral PH.

Several kinds of samples were studied, both suspensions and biofilms. The *B. cepacia* suspensions were introduced to Pb solutions at various pH levels, while a single-celled layer of *B. cepacia* on a substrate of α-Al_2O_3 (commonly known as sapphire) was grown for the biofilms. In addition to being a well-understood material, aluminum oxides are often found in contaminated soil and are highly reactive with heavy metals, making them an integral component of remediation. Researchers then either immersed the biofilm directly into a solution containing Pb or submitted the film to five minutes of x-rays to stop metabolic activity, and then introduced the Pb solution. The biofilms underwent x-ray fluorescence mapping at the GSE-CARS beamline 13-ID at the APS. X-ray absorption fine structure experiments were done on both the biofilms and the suspensions at the Stanford Synchrotron Radiation Laboratory.

Mapping of the biofilms that were x-ray treated showed a fairly homogeneous distribution of Pb uptake across the sample. The biofilms that had been allowed to retain metabolic activity, however, showed variations of up to an order of magnitude, with larger amounts of Pb collecting at various "hotspots" within the microcolonies (Fig. 1.).

Turning to the suspensions in order to better understand what was happening with the biofilms, x-ray absorption fine

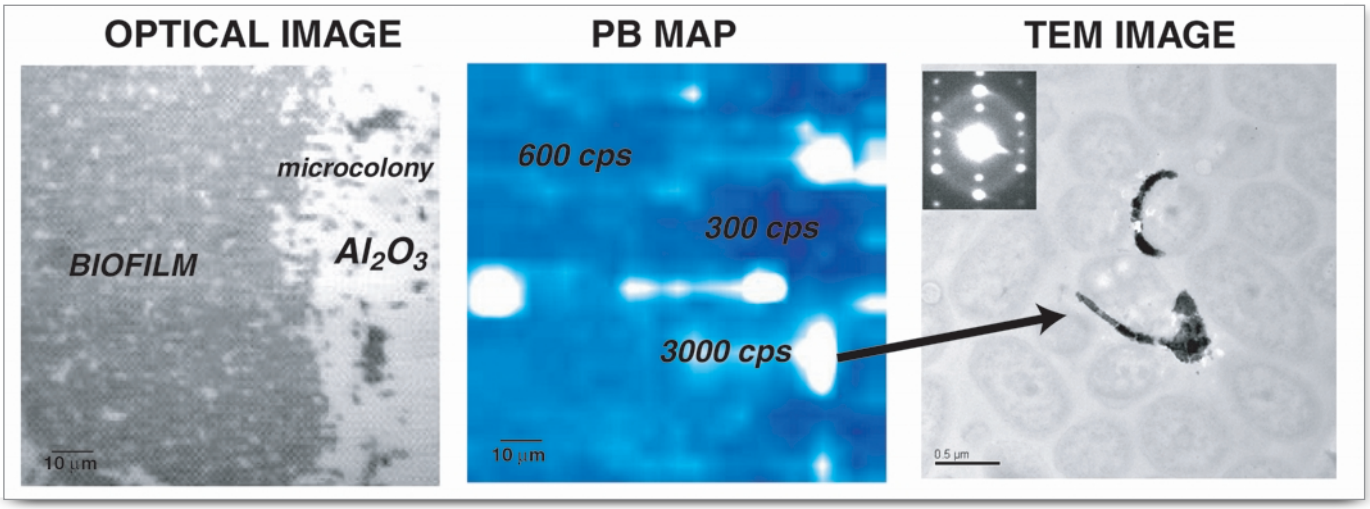

Fig. 1. Optical image and coupled Pb L_{III} x-ray fluorescence map (5 x 5-μm spot size) for a *B. cepacia* biofilm on α-Al_2O_3 incubated with 60-μm $Pb(NO_3)_2$ at pH 6. The false color scale from blue (300-cps Pb FY) to white (3000-cps Pb FY) shows the formation of Pb "hot-spots" in the biofilms. These hot-spots have been identified as Pb-phosphates (*e.g.*, pyromorphite) forming on the bacterial cell surfaces from TEM images (right) and GI-EXAFS spectra (data not shown).

structure (EXAFS) data showed that levels of adsorption and precipitation depend on pH. At low pH values, *e.g.*, pH 4, the EXAFS spectra matched those of the lead phosphate mineral pyromorphite ($Pb_5(PO_4)_3(OH)$), suggesting that the uptake is due to the formation of a precipitated form of Pb that is, at the very least, similar to pyromorphite. Subsequent transmission electron microscopy data showed that there was, indeed, pyromorphite present in the outer membrane of the *B. cepacia*. At low pH, the formation of pyromorphite accounts for 90% of the total Pb uptake. At higher pH, *e.g.,* pH 6, however, there is a mixture of sorbed Pb (42%) and biomineralized Pb (58%).

It is therefore hypothesized that similar adsorption and precipitation rates occurred within the biofilms. The films in which metabolic activity had ceased led solely to sorbed Pb, which was distributed evenly across the plate. In the remaining films, however, the "hotspots" were areas in which cells were substantially more biomineralized. These cells actively produce pyromorphite, incorporating the soluble form of Pb(II) as they do so, thus fixing it into place.

In the field, various characteristics affect the immobilization of toxic heavy metals. Different pHs, for one, affect sorption rates for different metals, and environmental chemists would like to predict which materials will provide the major repository for Pb at any given pH. This study shows that Pb binds to bacterial surfaces to a much greater extent at higher pH — and that such binding is all the more potent since it is through biomineralization, in addition to sorption. ❍

See: A.S. Templeton[1], T.P. Trainor[1,2], A.M. Spormann[1], M. Newville[2], S.R. Sutton[2], A. Dohnalkova[3], Y. Gorby[3], and G.E. Brown, Jr.[1,4], "Sorption versus Biomineralization of Pb(II) within *Burkholderia cepacia* Biofilms," Environ. Sci. Technol. **37**, 300-307 (2003).

Author affiliations: [1]Stanford University, [2]GSECARS, The University of Chicago [3]Pacific Northwest National Laboratory, [4]Stanford Synchrotron Radiation Laboratory

This work was supported by National Science Foundation (NSF) grants NSF-EAR-9905755 and NSF-CHE-0089215 and by the Eugene Holman Stanford Graduate Fellowship (A.S.T.). SSRL and the W.R. Wiley Environmental Molecular Sciences Laboratory (PNNL) are funded by the U.S. Department of Energy (Offices of Basic Energy Sciences and Biological and Environmental Research). SSRL is also funded by the National Institutes of Health. GSECARS is funded by the NSF (Earth Sciences Division) and by DOE (Geosciences Program). Use of the Advanced Photon Source was supported by the U.S. Department of Energy, Office of Science, Office of Basic Energy Sciences, under Contract No. W-31-109-Eng-38.